A NOTE ON THE INFLUENCE OF SHIELD GEOMETRY ON AIR DOSE AND TISSUE DOSE FROM PROTONS WITHIN A SPACE VEHICLE

Hermann J. Schaefer

JOINT REPORT

UNITED STATES NAVAL SCHOOL OF AVIATION MEDICINE

AND

NATIONAL AERONAUTICS AND SPACE ADMINISTRATION

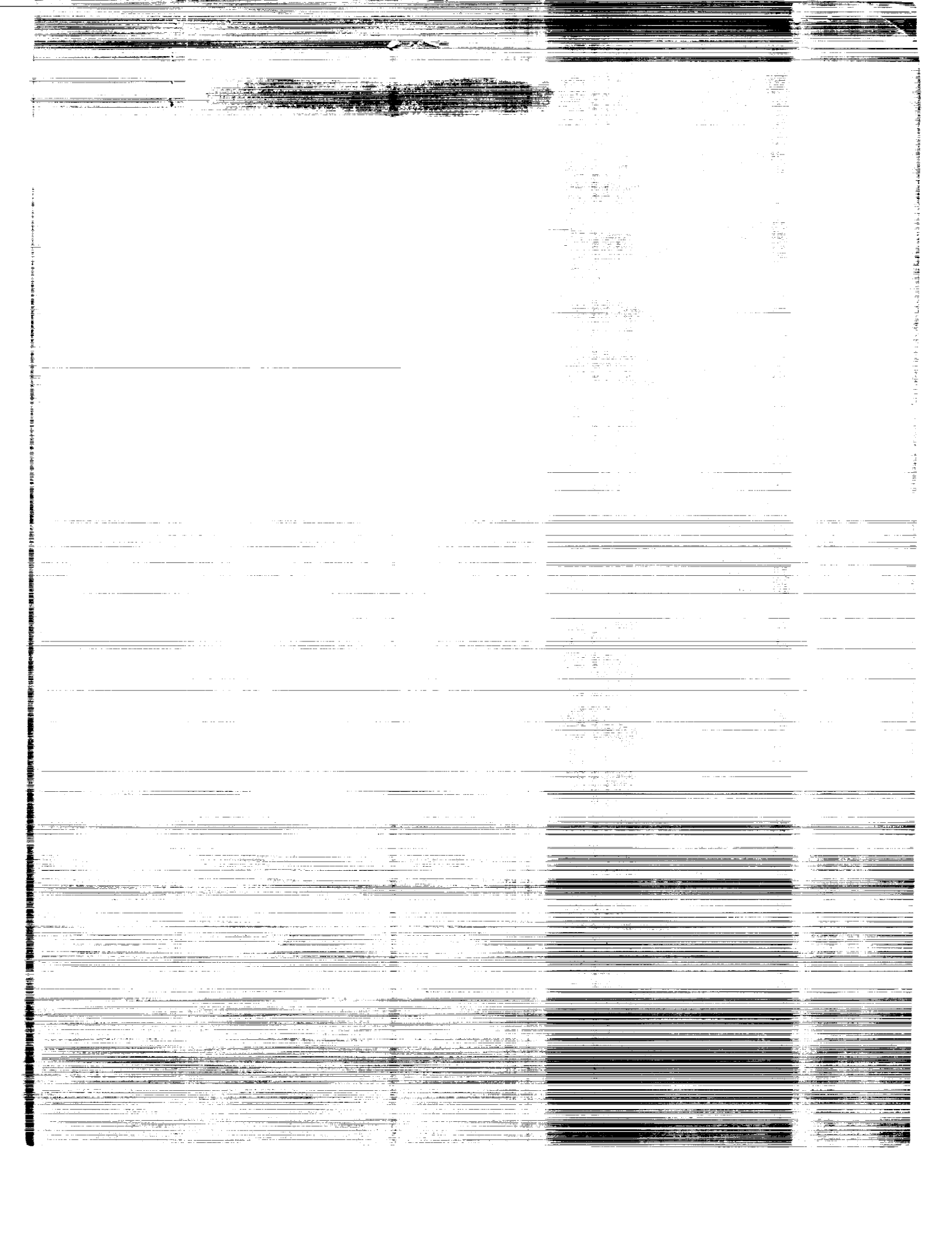

Research Report

A NOTE ON THE INFLUENCE OF SHIELD GEOMETRY ON AIR DOSE AND TISSUE DOSE FROM PROTONS WITHIN A SPACE VEHICLE

Hermann J. Schaefer

Bureau of Medicine and Surgery
Project MR005.13-1002
Subtask 1 Report No. 25

NASA Order R-75

Approved By

Captain Ashton Graybiel, MC USN
Director of Research

Released By

Captain Clifford P. Phoebus, MC USN
Commanding Officer

25 April 1963

U. S. NAVAL SCHOOL OF AVIATION MEDICINE
U. S. NAVAL AVIATION MEDICAL CENTER
PENSACOLA, FLORIDA

SUMMARY PAGE

THE PROBLEM

The dosage distribution within a closed vessel in proton radiation fields in space is highly structured because the spatial distribution of shielding material about a point in the vessel varies with location. In addition to vehicle frame and equipment, the body of the astronaut itself is part of the total shielding matter. The question arises as to what degree stationary radiation sensors measuring the distribution of air dose in the ship would allow inferences on the tissue dose in the astronaut's body.

FINDINGS

For three typical space radiation proton spectra, the distribution of air dose is analyzed computationally for a spherical shell of uniform wall thickness and for a conical vehicle carrying a heavy heat shield at the base. The results indicate that, even for the completely symmetrical spherical vessel, the air dose varies considerably at different radial locations due to the influence of shield geometry. For the ordinary cosmic ray beam, the local air dose is higher in regions where the effective shielding is heavier, contrary to flare produced and Van Allen Belt protons which show no build-up phenomenon.

For the conical vehicle, the computational analysis is extended to the dosage distribution within a spherical tissue phantom of 30 cm diameter assumed in two locations, in the nose tip and close to the heat shield. The results show that the depth dose distribution in the phantom differs greatly with regard to absolute level as well as to radial symmetry at the two locations. The corresponding air doses do not furnish any clues as to these differences. Specifically, greatly different tissue doses in the phantom can be found at locations at which the same air dose is measured.

It is concluded that accurate determination of the radiation exposure of the astronaut requires radiation monitors to be worn on the body. This seems all the more a logical solution since personal monitoring would be needed anyhow as soon as the astronaut wants to leave the vehicle. Additional stationary sensors in the vehicle still seem useful since they would indicate the directionality of the radiation and facilitate corrective action by attitude control or other means.

INTRODUCTION

Shielding the crew compartment of a space vehicle from ionizing radiation can be accomplished in a large part by making use of the inherent attenuating power of construction material and equipment. Quite obviously, on the other hand, the utilization of this principle has its limitations. It will not be possible, for example, to distribute the weight completely uniformly around the compartment to be shielded. There will always be "windows" where the inherent shielding is less than average as well as other sections where shielding is exceptionally heavy. In any vehicle designed for re-entry, the heat shield in particular will offer a disproportionately heavier shielding to incident radiation than the rest of the vehicle frame.

The picture becomes further complicated if, for a given geometrical arrangement of the total matter of a ship, the attenuation mechanism of the radiation is taken into consideration. Contrary to ordinary cosmic radiation, the various high intensity radiation beams in space contain large fractions of particles of comparatively low penetrating power. The local radiation intensity within a ship, therefore, depends in a complex fashion on both the geometrical shield configuration and the physical characteristics of the radiation. It can be expected that there will be "hot, warm, and cool" places inside a ship traversing the Van Allen Belt or a solar particle beam. A closer assessment of the quantitative aspects of these relationships seems of special interest. The following treatise is an attempt in this direction. It is limited in its scope to protons since this type of radiation seems to constitute by far the greatest potential hazard for acute radiation injury in space flight.

BASIC TYPES OF PROTON RADIATIONS IN SPACE

The various types of proton radiation beams in space differ greatly with regard to their energy spectra, i.e., their penetrating power. At the lower end we find flare produced protons with energy spectra of a steep negative slope with very high flux values at low penetrating powers, yet with a moderate or small fraction of particles of high penetration. At the upper end we find the proton component of the ordinary cosmic ray beam with particles of tremendous penetrating power, but of such a low flux value that they pose no acute radiation hazard.

In view of this wide variety of spectral configuration, it seems advisable to analyze the influence of geometrical factors on the radiation field within the vehicle for several representative spectra. Throughout the following study, data have been established for three basic spectra. Two of them have been investigated in an earlier study (1) with regard to depth dose distribution in a tissue phantom. Spectrum I has been proposed by Bailey (2) as representative for a typical large flare event. It is based on a synoptic evaluation of data of independent observers, pertaining mainly to the giant flare of February 23, 1956. With the restriction that it might be

exceeded on rare occasions, it can be considered a maximum event for assessing shielding requirements in general. Spectrum II is representative for the proton flux in the Van Allen Belt as communicated by Freden and White (3). It represents the transitional type of energy spectrum in which the flux in the region of several hundred million e-volts energy becomes substantial. Finally, Spectrum III represents the ordinary cosmic ray beam. It is the extreme case in which the bulk of the particle flux is found in the region of one billion e-volts and beyond. As will be shown presently, the shielding effect for this spectrum is, for a considerable interval of light and medium heavy shielding, reversed. That means, the exposure closely behind a heavier shield is higher due to the build-up of secondaries in the shield. Spectrum III, to a certain extent, also could be considered as representative of the so-called Prompt Spectrum immediately after a relativistic flare of the rare type mentioned above.

In analyzing intratarget dose distributions, the energy spectrum is not a very meaningful way of describing the characteristics of a given radiation. Since energy and range are connected by a strongly nonlinear relationship, the E-spectrum does not convey direct information on penetrating power. The latter quality is described much better by means of the depth dose curve which a parallel beam of the radiation in question would produce in a slab of absorption material entering it at right angle. For the three types of proton radiations selected for the present study, the pertinent curves are shown in Figure 1. It is seen that they cover a very wide range of penetrating powers.

Of special interest is the depth dose distribution of the ordinary cosmic ray beam. It is based on the altitude profile of the total ionization in the earth's atmosphere which has been measured repeatedly. The reader is especially referred to the work of Neher (4). In using data on the total ionization of cosmic radiation for the purpose of the present study one has to be aware of a basic difference in the directionality of the radiation. Primary cosmic ray particles enter the atmosphere of the earth from the 2 pi solid angle of the upper hemisphere from all directions. The curves in Figure 1, however, pertain to the depth dose distribution as it would develop from a unidirectional beam of vertical incidence. This is an essential prerequisite since the data of Figure 1 are to be used, in the present study, as representative for differential unidirectional beams to be integrated over the entire solid angle of the sky. This integration will ultimately furnish the depth dose distribution in a given compact target. Because of the great complexity of attenuation and production of secondaries of primary cosmic ray particles in the atmosphere, no experimental method exists which would allow reconstructing, from the altitude profile of the total ionization, the underlying depth dose curve of a unidirectional primary cosmic ray beam. However, if the assumption is made that all secondaries produced in interactions of primaries with nuclei of the absorber material are emitted

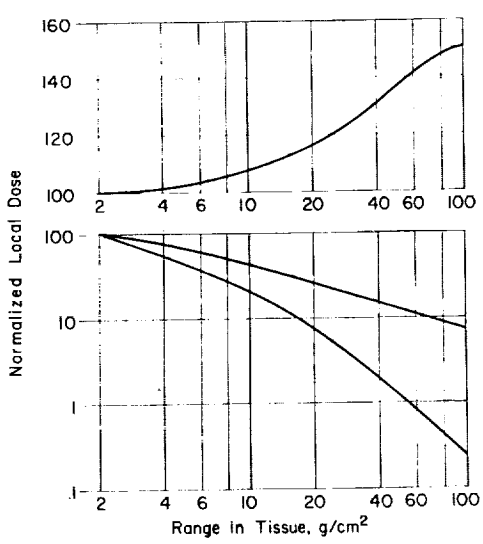

Figure 1

Penetrating Power of Three Spectral Types of Proton Radiations Used in the Present Analysis

Shown is local dose for a parallel beam entering a slab of tissue at right angle.

in forward direction in the line of travel of the primary, one can establish, in successive approximations, a fictitious unidirectional differential cosmic ray beam which furnishes, if numerically integrated over 2 pi, the actual altitude profile of the total ionization in the atmosphere. Admittedly, this disregard of the lateral expansion of the photo-electron and nuclear cascades limits the validity of the model sharply as far as really accurate dose estimates are concerned. On the other side, it appears quite acceptable as a first approximation estimate in the present context inasmuch as it overrenders the build-up phenomenon, i.e., relative depth doses.

Another objection against the transfer of data which hold for the upper atmosphere to a compact absorber of density of 1.0 could be raised by pointing to the fact that, in dense matter, charged pi mesons will undergo nuclear collisions whereas in the upper atmosphere they will predominantly decay before they have a chance of nuclear interaction because of their extremely short lifetime. However,

this difference pertains to only one of the many types of secondaries which cosmic ray primaries produce in the atmosphere. Therefore, it affects the build-up phenomenon only to a minor degree and need not be considered in a first approximation analysis.

Quite generally the production of secondaries in nuclear collision is a process competing with ordinary ionization in the attenuation of high energy protons. The two mechanisms of energy dissipation are basically different and show a greatly different dependence on kinetic energy of the primary particle. As compared to ordinary ionization, nuclear collision makes itself felt as a contributing factor to the total energy dissipation only from energies of about 100 Mev on up. In an earlier study (5) these relationships have been analyzed in more detail. It was shown there that for Spectrum I nuclear collision can be disregarded in assessing depth dose distributions unless exceptionally heavy scattering masses of the order of tons are involved. For Spectrum II, the relative share of protons in the energy region of several hundred Mev is substantially larger than for Spectrum I. Wilson, Miller, and Kloster (6) have determined, for Spectrum II, the dose contributions from secondary protons and cascade and evaporation neutrons. They arrived at a depth dose distribution which shows essentially the same slope as the corresponding curve for Spectrum II in Figure 1 on which the following analysis is based.

Before a discussion of the main problem is started, a question of terminology has to be settled. In the dosimetry of ionizing radiations, dose or dose rate in a radiation beam or field can be determined in two different ways. They can be measured at the point of interest, usually with an air or tissue equivalent thimble chamber, without or with the object to be irradiated present. The two doses will generally be different because of the additional absorption and scattering produced by the irradiated object as compared to the situation in free air. In the older terminology, the two magnitudes in question have been denoted with the very descriptive terms "air dose" and "tissue dose." The official terms to be used now as decided by the International Commission on Radiological Units (7) are "exposure" and "absorbed dose." It should be noted that the ICRU has defined these expressions mainly for x- or gamma rays. Systematic dosimetric experiments concerning proton radiations with omnidirectional incidence and continuous energy spectra as they are encountered in space have not been carried out as yet. Existing knowledge concerning the attenuation mechanism of protons readily suggests that the conditions in x- or gamma radiation fields cannot be schematically transferred to protons. In fact, the present study tries to argue this very point. In view of this situation and since it was felt that an attempt at applying official terminology to a new and as yet unexplored area should not be undertaken at this early time, the following treatise uses the terms "air dose" and "tissue dose." As they have been deleted from the glossary of official terminology, they no longer carry any restricted meaning and seem the logical choice for the present treatise.

THE GEOMETRICAL FACTOR

An example of the influence of the geometrical factor on effective shield thickness within a closed vessel is described in the sketch of Figure 2. Let a spherical shell of 2 g/cm^2 uniform thickness be considered as a coarse model of the frame of a space vehicle. It is seen by inspection that only in the exact center of the vessel is the effective shield thickness equal to the actual thickness of 2 g/cm^2 for all directions of arrival of radiation from the outside. For an eccentrically located point inside the vehicle the effective shield thickness equals 2 g/cm^2 only in the two directions of the central diameter through the point. For all other

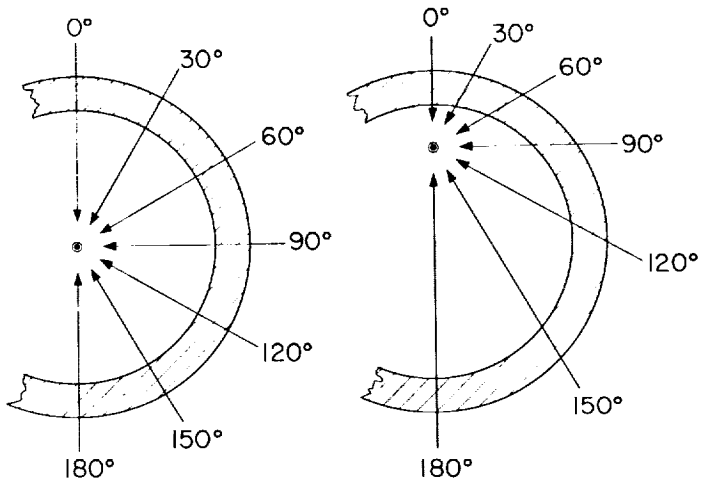

Figure 2

Influence of Shield Geometry on Effective Shield Thickness for a Spherical Vessel

Left: In the center, effective shield thickness and actual wall thickness are equal for all directions of arrival.

Right: At eccentric locations, effective shield thickness is always larger than actual wall thickness except for 0° and 180° incidence.

directions, incident radiation will pass through a larger effective shield thickness because of oblique incidence. It is easily seen that this effect is largest for a point directly on the inner surface of the shell and for a direction of incidence tangential to the inner surface.

The geometrical analysis of the problem is quite simple and leads to an angular dependence of effective shield thickness on direction of incidence for eccentrically located points, as shown in Figure 3. The left hand graph defines the radial distance, d, from the center. The two right hand graphs show the dependence of effective shield thickness on zenith angle of incidence for lower (upper graph) and higher (lower graph) values of d. It is seen that the effect

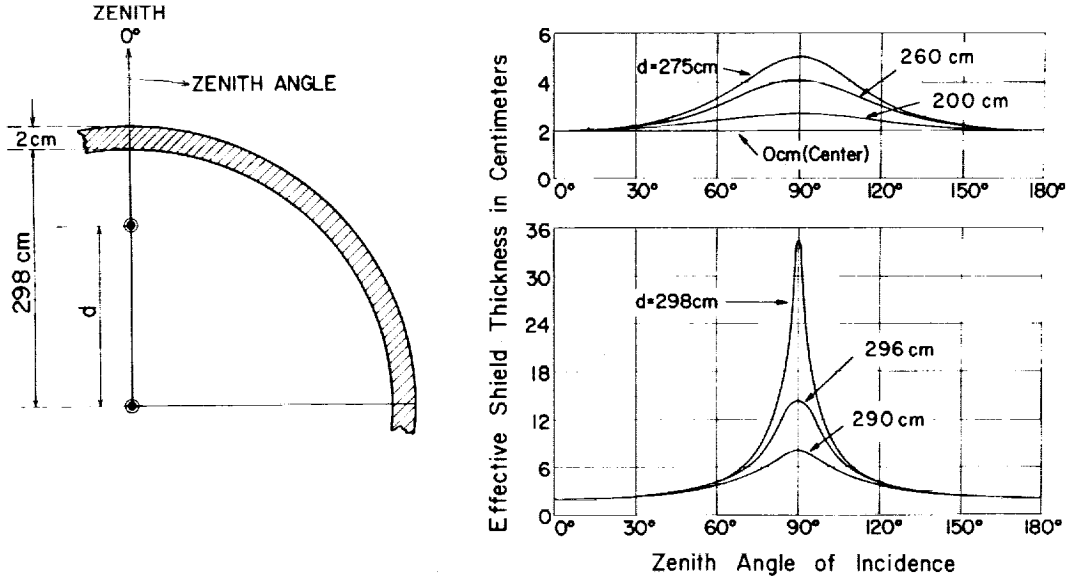

Figure 3

Effective Shield Thickness as a Function of Angle of Incidence in a Spherical Shell for Various Radial Locations

develops slowly as location moves radially outward assuming larger proportions only when a radial distance of about 2/3 of the full radius is reached. It is seen that, for angles of incidence closely below and above 90°, the effect becomes very large, reaching a maximum of 34.6 g/cm^2 effective shield thickness for a point directly on the inner surface and for 90° incidence. That means that shield thickness is enlarged by a factor of about 17. However, it is also seen that these extreme increases are limited to a narrow angular interval. In other words, the advantage of this exceptional gain in protective power is confined to a small ring-shaped solid angle of incidence. As a consequence, the reduction in total dose at such peripheral points within a spherical vessel can be expected to be only moderate for omnidirectionally incident radiation.

The foregoing discussion was carried out, for better descriptiveness, for a vessel of 300 centimeters radius. By expressing wall thickness as well as radial position of the point of observation in fractions of the full shell radius the variables and parameters of the system can be normalized. This procedure leads to exactly the same family of curves shown in Figure 3, merely with changed notations. A simple scaling law allows reading, from such a normalized set of curves, the effective shield thickness in absolute terms for spherical shells of any radius and any angle of incidence.

INFLUENCE OF GEOMETRICAL FACTOR AND ATTENUATION CHARACTERISTICS ON THE RADIATION FIELD WITHIN THE VEHICLE

THE SPHERICAL SHELL

The relationships described in the preceding section are quite trivial and well known in the design of radiation shields. For space radiation protons they assume special significance because of the peculiar attenuation characteristics of these beams. It should need no further explanation that, for heterogeneous radiations containing components of different penetration with varying flux values, it is not possible to determine, for a given point in a given vessel, a general equivalent mean shield thickness for omnidirectional incidence. Comparing the curves of Figure 3 showing the influence of the geometrical factor on effective shield thickness and those of Figure 1 showing the attenuation for various unidirectional beams, one sees that the resulting integral dose at an eccentrically located point within the vessel depends in a complex fashion on both the angular distribution function of the effective shield thickness and on the particular attenuation function of the radiation to be investigated. Breaking down the 4 pi solid angle of the sky in small facets and establishing the attenuation for each facet furnishes differential contributions which, by numerical integration, yield the resulting local dose. In comparing various spectral types of radiations, these local doses should preferably be normalized in order to allow a direct comparison.

The results of the indicated evaluation for the three spectra under discussion and for the spherical vessel of Figure 3 are shown in Figure 4. Plotted are normalized local exposure on the ordinate and radial distance from the center of the shell on the abscissa. Exposure is expressed in terms of air dose rate. That means the ordinate indicates the dose rate which an air equivalent small ion chamber freely exposed at the point of observation would show. It is seen that the exposure varies

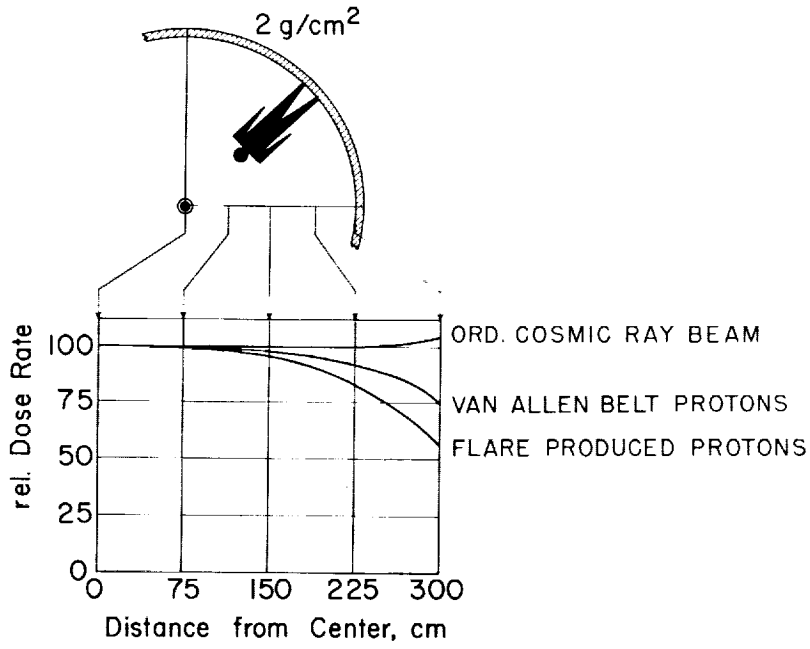

Figure 4

Normalized Air Dose Rates in a Spherical Shell of 300 cm Radius and 2 g/cm² Wall Thickness as a Function of Radial Exposure for Three Basic Proton Radiations

considerably within the vessel, dropping substantially toward the periphery. The effect is most pronounced for Spectrum I because it shows the steepest negative slope; i.e., it is the most heterogeneous spectrum. Immediately at the inner surface the exposure amounts, for this spectrum, to only 55 per cent of that in the center. For Spectrum II the effect is less pronounced than for Spectrum I, yet still sizeable in absolute terms with a minimum dose at the inner surface of 75 per cent. For both spectra a substantial gain in protective power does not set in until half the full radial distance from the center is passed. Finally, Spectrum III, the representative spectrum of the ordinary cosmic ray beam, shows a reversed effect. The dose is smallest in the center and increases, though only slightly, toward the periphery as the effective shielding becomes heavier.

A human target is drawn to scale in Figure 4. It is seen that the air dose rate varies indeed quite substantially for different parts of the body. It has to be realized, however, that self-shielding of such a human target produces additional complex changes of the dosage distribution in the vehicle both inside as well as outside the human target. A mere analysis of the air dose in an otherwise empty vehicle, therefore, is an inadequate analysis if actual information on tissue dosages is desired.

The influence of the shield geometry on the radiation field within a closed vessel could be described in a most general way by stating that directionality of the incident radiation is altered. In particular, an omnidirectionally isotropic incident radiation becomes anisotropic within a closed vessel. As a consequence, the ionization dose at a given location within a compact target (e.g., lenses of the eyes of the astronaut) depends not only on the geometry of the external shielding, but also on orientation of the target in the vessel. It seems of interest to demonstrate this effect with a special example.

CONICAL VEHICLE WITH HEAT SHIELD

Because of its high symmetry, the spherical shell discussed in the preceding section has the advantage that it is easily analyzed, yet it is not a very close approximation of an actual vehicle frame. A better system in this respect is the conical vehicle shown in the left part of Figure 5. Though still a greatly simplified model it simulates at least the basic shape of an actual vehicle. The geometrical analysis of this system is vastly more complicated than that of a spherical shell if a full evaluation of the dosage field inside is desired. However, sufficient information can be obtained if the exposure along the central axis of the vessel is determined. For this axis, directional attenuation varies only with zenith or nadir angles, but not with azimuth angle. This greatly reduces the computational work load.

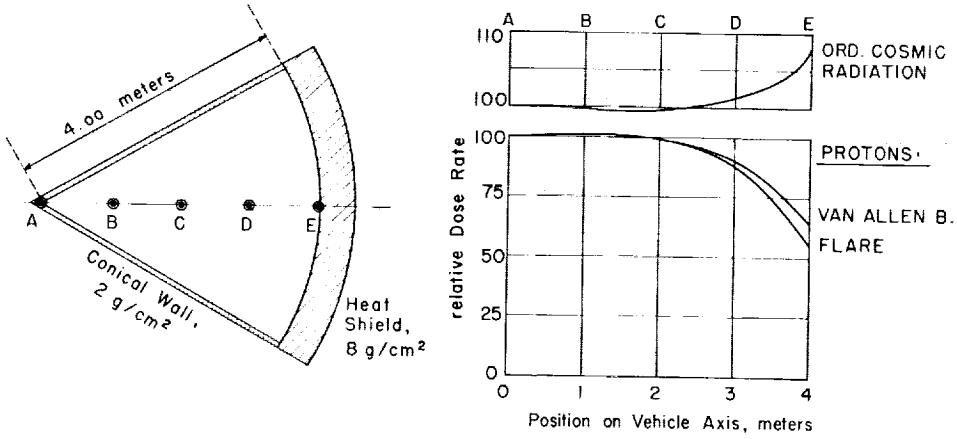

Figure 5

Effect of Shield Geometry on Local Air Dose in a Conical Vehicle With Heat Shield

Left: Simplified model of large conical space vehicle.

Right: Normalized air dose rates along axis of vehicle for three basic proton radiations.

The graph of Figure 5 shows normalized exposure in air along the central axis for three spectra. The curves hold for a thickness of the conical wall of 2 g/cm^2 and of the spherical heat shield of 8 g/cm^2. Contrary to the spherical vessel, highest exposures do not prevail at a geometrically well-defined point in the system but occur on the central axis at points in the vicinity of, yet a finite distance away from, the nose tip, with exact location varying slightly with spectral configuration. For the ordinary cosmic ray spectrum, relationships are again reversed and minimum exposure occurs at the corresponding point. The curves of Figure 5 are normalized by setting the doses directly on the inner surface in the nose tip of the vessel equal to 100. It is seen that, for flare produced and Van Allen Belt protons, the exposure drops substantially toward the heavy heat shield, reaching a minimum directly on the inner surface of the heat shield whereas the cosmic ray beam shows the reversed trend.

As pointed out before, the air dose distribution within a closed vessel does not allow a direct inference on the absorbed dose in a compact target. The curves in Figure 5, therefore, need to be supplemented for an evaluation of the dosage distribution in a target at different locations within the vessel. For this analysis, a spherical tissue phantom of 30 cm diameter has been assumed once positioned in the nose tip (Position NT) and once directly at the heat shield (Position HS), as indicated in the left hand sketches of Figures 6 and 7. The depth dose distribution along the central diameter of the tissue sphere coinciding with the vehicle axis is shown in Figure 6 for flare produced protons for Position NT and HS. As a comparison, the corresponding depth dose distribution as it would develop in the same phantom for central position in a spherical shell of a uniform wall thickness of 2 g/cm^2 throughout and of very large radius is also shown. The essential feature is the much greater asymmetry of the depth dose pattern for Position HS as compared to Position NT. For Position NT, the surface dose in the tissue sphere at the point

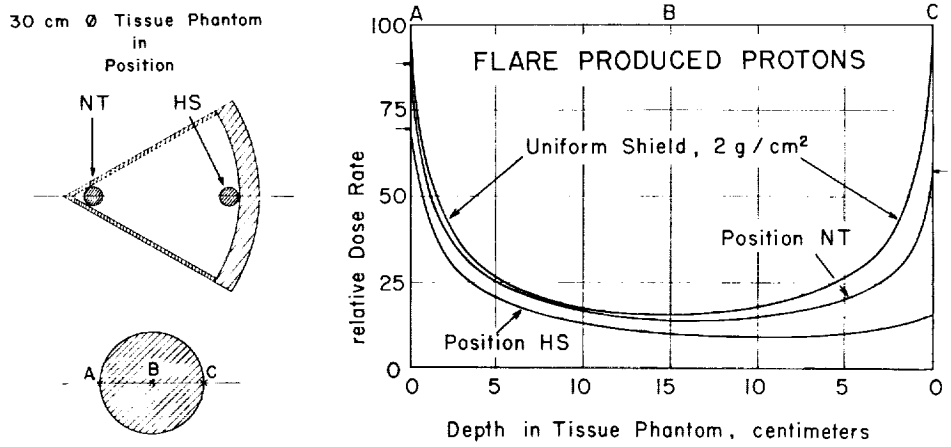

Figure 6

Depth Dose Distribution in 30 cm Diameter Tissue Sphere Along Axis at Two Different Locations in Conical Vehicle for Flare Produced Proton Radiation

Dose rates are normalized to surface dose in same phantom for central location in spherical shell of Figure 4.

toward the nose tip equals 88 per cent as compared to 57 per cent for the opposite surface point toward the heat shield. For Position HS the corresponding doses are 69 per cent and 15 per cent, respectively. These values indicate that, in the vicinity of the heat shield, not only the radiation exposure is reduced, but also a completely different depth dose pattern is obtained. This effect is not due to an actual change of penetrating power of the radiation within the vessel but is an outcome of strong directional asymmetry of incidence.

The point in question might be elucidated with a concrete example. An astronaut with his head in the nose tip could slightly reduce the exposure of the lenses of his eyes in a solar particle beam by turning his head in the proper direction, namely, toward the heat shield. With his head close to the heat shield, however, he could very substantially reduce exposure of his lenses by the same head motion. In other words, at one location in the ship, exposure depends strongly on directional position and at another location it does so only very little. It is quite obvious that this peculiar difference cannot be gathered from the air dose values as such at the locations in question. This must not necessarily mean that stationary radiation sensors measuring air doses at suitably chosen places in a larger ship or space platform would not fulfill a useful function as will be discussed later.

Figure 7 shows the tissue dose for the same system as Figure 6 but for Spectrum II. To be sure, if Spectrum II is interpreted as representative for the proton flux in the Van Allen Belt, the objection might be raised that the assumption of omnidirectional isotropy of incidence is not correct. A large part of the flux in the magnetosphere shows cylindrical symmetry. Obviously, the shield geometry would affect the radiation field inside the vehicle, as far as both the air dose and the tissue dose in a compact target are concerned, in a completely different way. For this reason it seems more appropriate to consider Spectrum II in this particular context as another type of flare produced proton radiation which carries a significantly larger relative share of particles in the energy region of several hundred Mev. As pointed out above, these types of flare spectra do occur. Since they pose a more serious hazard in view of their higher penetrating power, the data of Figure 7 seem of definite interest. They show that the directional effect producing a strongly asymmetrical dose distribution in the tissue phantom in Position HS is fully developed also for this radiation. Merely the relative depth doses are substantially larger for Spectrum II because of a larger relative share of particles of higher penetration.

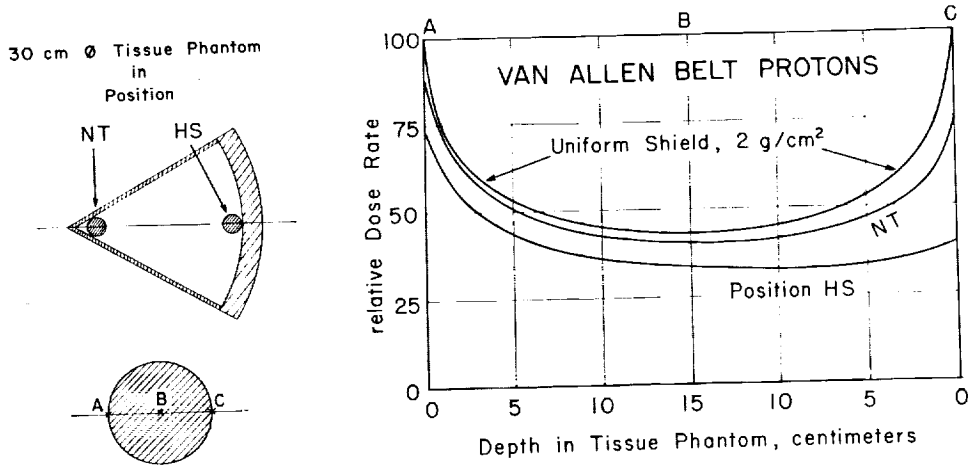

Figure 7

Depth Dose Distribution in 30 cm Diameter Tissue Sphere Along Axis at Two Different Locations in Conical Vehicle for Proton Radiation in the Van Allen Belt

For normalization see note under Figure 6.

CONCLUSIONS

The main conclusion to be drawn from the results of the analysis presented can be worded quite concisely. Measurement of air doses in a closed vessel exposed to proton radiation fields in space, even if carried out at several different locations, does not furnish meaningful information on tissue doses that would develop in a compact target at these locations. Not even the surface doses in such a target could be correctly inferred from air dose measurements. Depending on shield geometry, surface and depth dose in a human target can vary greatly at two different locations in the vessel at which the same air dose is recorded. Said doses can even be different at the same location in the ship for different orientations of the target. It is seen, then, that a realistic determination of the radiation exposure of an astronaut would actually require radiation sensors on his body. Since such sensors will be needed anyhow as soon as the astronaut wants to leave the ship, be it in orbit or on the moon, one might conclude that it is simplier to wear them all the time. In regard to this argument it should be pointed out that stationary sensors at different locations in the ship could still be of great value. Particularly in a larger ship offering some freedom of locomotion and body positioning for the crew, monitoring of the radiation field in the ship in flight through a solar particle beam or through the Van Allen Belt would

convey rapid information on the directionality and general distribution of the radiation. It would enable the astronaut at the controls to minimize exposure by correcting the attitude of the vehicle in relation to the incident beam. This is of special importance in the vicinity of the earth where the incident radiation is always strongly directional, and quick corrective action could substantially reduce the exposure.

A determining factor as to the instrumentation needed would also seem to be the degree of accuracy which one would consider necessary for the measurement of the radiation exposure of the astronaut. As long as the integral exposure remains below the level of acute injury, a well-designed system of stationary radiation sensors would seem sufficient for an actual space mission. It is felt, however, that this could be finally decided only on the basis of more elaborate data requiring direct measurements with phantoms in satellites. The theoretical study presented here can only define the problem and describe the basic phenomena involved. The real radiation field in a vehicle in flight through a solar particle beam is vastly more complicated than the simple patterns arrived at above. This field reflects the enormous complexity of the equipment in the ship producing an equally complex distribution of effective shield thicknesses for different directions of incidence which, in turn, is finally reflected in the dose rate distribution. How far it can be simplified for in-flight interpretation by the astronaut and still be meaningful would seem to require extensive further studies.

REFERENCES

1. Schaefer, H. J., Dosimetry of proton radiation in space. BuMed Project MR005.13-1002 Subtask 1, Report No. 19. Pensacola, Fla.: U. S. Naval School of Aviation Medicine, 1961.

2. Bailey, D. K., Time variations of the energy spectrum of solar cosmic rays in relation to the radiation hazard in space. J. geophys. Res., 67: 391-396, 1962.

3. Freden, S. C., and White, R. S., Particle fluxes in the inner radiation belt. J. geophys. Res., 65: 1377-1383, 1960.

4. Neher, H. V., and Anderson, H. R., Cosmic rays at balloon altitudes and the solar cycle. J. geophys. Res., 67: 1309-1315, 1962.

5. Schaefer, H. J., A note on the influence of nuclear collision on the radiation dose from flare produced protons in space. BuMed Project MR005.13-1002 Subtask 1, Report No. 23. Pensacola, Fla.: U. S. Naval School of Aviation Medicine, 1962.

6. Wilson, R. K., Miller, R. A., and Kloster, R. L., A study of space radiation shielding problems for manned vehicles. Contract No. NAS5-1093. FZK-144. Fort Worth, Texas: General Dynamics, 1962.

7. International Commission on Radiological Units and Measurements, Radiation quantities and units. Report 10a. Handbook 84. Washington, D. C.: National Bureau of Standards, 1962.